

Interrupted tubules in filamentous crystals: Elastic analysis

M. Upmanyu

Simulation and Theory of Atomic-scale Material Phenomena (stAMP), Materials Science Program, Engineering Division, Colorado School of Mines, Golden, Colorado 80401-1887, USA

J. R. Barber

Department of Mechanical Engineering, University of Michigan, Ann Arbor, Michigan 48105-1887, USA
(Received 25 February 2005; revised manuscript received 30 August 2005; published 30 November 2005)

We have performed a linear elastic analysis of an interrupted tubule (IT) in a transversely isotropic, crystalline filamentous crystal. Elastic solutions for stresses, strains, and displacements are derived using the inherent antisymmetry about the plane of the IT defect. We show that the solutions can be expressed in terms of two related strain potentials evaluated in different transformed coordinate systems. The displacements are long range and the defects accumulate significant strain energy. We extend our elastic analysis to IT defects in crystalline nanotube ropes (CNTR), where the coupled coordinate systems are necessarily real. We find that the stresses diverge within a dumbbell-shaped core region, and the core shape is sensitive to the tube radius. Finally, we discuss finite-size effects and registry-dependent modifications to the analysis.

DOI: [10.1103/PhysRevB.72.205442](https://doi.org/10.1103/PhysRevB.72.205442)

PACS number(s): 61.72.Bb, 61.48.+c, 62.20.Dc, 87.16.Ka

I. INTRODUCTION

Aggregates of filaments often assemble to form single crystals, where interfilament cohesive forces result in transversely isotropic assemblies of hexagonally packed filaments. Examples include crystalline nanotube ropes (CNTRs),¹ and nanowire assemblies, actin filaments,^{2,3} sickle haemoglobin (HbS) fibers,⁴ hexatic phase in polymeric liquid crystals,⁵ micelle assemblies,⁶ squid rhodopsin,⁷ etc. The properties of these aggregates are largely due to interfilament alignment, and are therefore sensitive to crystalline defects that break the symmetry of the hexagonally packed crystals. A fundamental understanding of thermodynamics and kinetics of these defects is important for understanding the structure–property relations in these crystals, and also to modify and eventually tailor their functionality for bionanotechnological applications.

As in atomic/molecular crystals, the aggregate can consist of single filament (equivalent to point defects), line, planar, and bulk defects. Here, we present on elastic analysis of a novel class of defects that do not have counterparts in conventional crystals, i.e., interrupted tubules (IT defects or \odot) in an otherwise infinite filamentous crystal (see Fig. 1). These are single filament defects in 3D filament assemblies (equivalent to a “point dislocation”), and 2D edge dislocations in single layer assemblies.⁹ They can form due to varying assembly conditions; mismatch in filament aspect ratios, unfavorable growth conditions at single or multiple filaments, induced interfilament sliding, etc. They can also occur as multiple ITs, when open ends of two or more growing filaments combine to form “hairpinlike” terminated ends.

In assemblies of continuous filaments, the IT defect is intrinsically sessile as its motion is constrained along the filament axis, which in turn requires external forces acting on the interrupted tubule. On the other hand, in systems where each filament itself is a loose aggregate (monomeric) of subunits, the IT defect can move in the interrupted plane (x - y plane in the schematic) via attachment-detachment-limited

transfer of the filament subunits, analogous to bonding-debonding associated with the glide of dislocations on their slip plane.⁹ Additionally, the IT defect can also climb along its axis via diffusion of the subunits to and from the interrupted end of the IT defect. Therefore, we expect these defects to be mobile in several of the naturally occurring assemblies (actin filaments, HbS fibers, micelle assemblies), and also synthetic assemblies such as liquid crystals and high-temperature polymer aggregates.

IT defects will also modify thermomechanical and transport properties of the aggregate.¹⁰ For example, it has been speculated that the localized strain fields due to the disruption in symmetry modify interfilament sliding behavior and therefore affect the bulk flexural response of nanotube ropes.¹⁰ They can also act as vortices of trapped carriers of bulk fields and gradient currents, quite like splay defects in polymeric liquid crystals.⁵ The modifications in the mechanical and transport properties can also serve as regulatory sig-

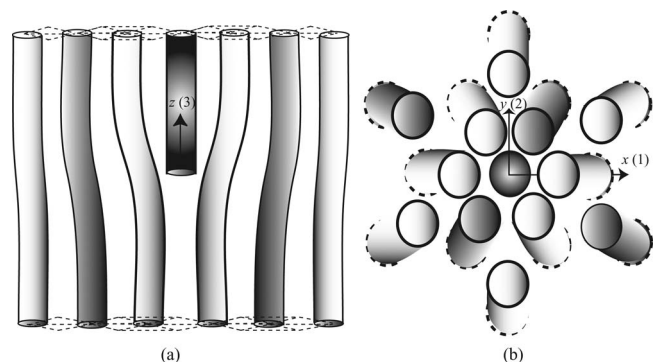


FIG. 1. Schematic of interrupted tubule (IT) in an otherwise perfect one-dimensional crystalline assembly of filaments. (a) Longitudinal view of the layer containing the IT defect and (b) the transverse view between two z planes sandwiching the IT. The shading indicates registry-dependent orientational order, with a repeat unit of two nanotubes (Ref. 8).

nals that control the aggregation/polymerization of individual filaments during crystal growth.

Here, we focus on the elastic field associated with these defects. The analysis presented here is limited to IT defects in elastically stiff filamentous crystals, where the persistence length of bending ($l_b = EI/k_B T$) and twisting ($l_t = GJ/k_B T$) of individual filaments is much larger than the extent of the strain fields associated with the IT defect (EI and GJ are the bend and torsional stiffness of the filaments). The primary focus is on IT defects in CNTRs, where structural studies have shown at small tube radii ($< 25 \text{ \AA}$), weak van der Waals internanotube interactions result in hexagonally packed cross sections. These bulk crystalline nanomaterials have been grown using bulk applied fields¹ and self-assembly.^{11–14} CNTRs have lately attracted interest due to their significantly superior yet transversely isotropic mechanical^{10,15} and transport properties—thermoelectric power generation,¹⁶ hydrogen sorption,¹⁷ superconductivity,¹⁸ field emission displays,¹⁹ etc.

In the following sections, we develop expressions for elastic stresses and strains due to these defects in infinite 3D filamentous crystals, within the framework of transversely isotropic linear elasticity. We first derive the general solutions for an arbitrary, transversely isotropic crystalline assembly, and then apply the analysis to CNTRs. The effect of radius of nanotubes forming the CNTRs is also analyzed. Finally, refinements to the elastic solutions due to finite size of these aggregates and registry dependent inter-filament interactions are discussed.

II. ELASTIC ANALYSIS

A. The boundary value problem

IT defects result in a displacement discontinuity across the two transversely isotropic elastic half-spaces joined at the plane normal to the filament axis and passing through the terminated end of the interrupted tubule. Setting the origin at the terminated end of the IT and the z axis along C_h , the displacement discontinuity is now across the $z=0$ plane. The strength of the IT, the amount of extra material that must be inserted along the z axis to restore continuity, can be defined in terms of an IT vector $\mathbf{a}_\odot = a_\odot \hat{\mathbf{r}}$. This displacement is required to complete any cylindrical circuit across the $z=0$ plane, analogous to the well-known Burgers vectors and circuits associated with dislocations.⁹ That is,

$$u_r(r, 0^+) - u_r(r, 0^-) = a_\odot. \quad (1)$$

Evidently, $a_\odot = \chi r_0$, where r_0 is the equilibrium interfilament spacing in the underlying hexagonal lattice and χ is an integer. $\chi=1$ for a single IT and $\chi>1$ for multiple ITs. The displacements are axisymmetric, i.e., $u_\theta=0$, $u_r \equiv u_r(r, z)$, and $u_z \equiv u_z(r, z)$. Also, due to antisymmetry about the $z=0$ plane,

$$u_r(r, 0^-) = -u_r(r, 0^+). \quad (2)$$

Combining Eqs. (1) and (2),

$$u_r(r, 0^+) = \frac{a_\odot}{2}. \quad (3)$$

Antisymmetry also requires that

$$\sigma_{zz}(r, 0^+) = 0. \quad (4)$$

Equations (3) and (4), together with “infinity boundary conditions” (the stresses and strains approach zero as $r \rightarrow \infty$ and $z \rightarrow \infty$) completely specify the problem in the elastic half-space $z > 0$.

B. Formulation of the problem

In the remainder of this section, we develop the elastic solution using strain potentials and harmonic functions, similar to those used in isotropic elasticity. Following Ting,²⁰ we define a mapping $z = \lambda \zeta$, where λ is a constant. The displacement $\mathbf{u} \equiv (u_x, u_y, u_z)$ can be defined as the gradient of a scalar function ϕ ,

$$u_x = \frac{\partial \phi}{\partial x}, \quad u_y = \frac{\partial \phi}{\partial y}, \quad \text{and} \quad u_z = \frac{\partial \phi}{\partial \zeta} = \lambda \frac{\partial \phi}{\partial z}.$$

The strain components can then be constructed,

$$\begin{aligned} e_{xx} &= \frac{\partial^2 \phi}{\partial x^2}, & e_{yy} &= \frac{\partial^2 \phi}{\partial y^2}, & e_{zz} &= \lambda \frac{\partial^2 \phi}{\partial z^2}, \\ e_{yz} &= \frac{(1+\lambda)}{2} \frac{\partial^2 \phi}{\partial y \partial z}, & e_{zx} &= \frac{(1+\lambda)}{2} \frac{\partial^2 \phi}{\partial z \partial x}, \\ e_{xy} &= \frac{\partial^2 \phi}{\partial x \partial y}. \end{aligned} \quad (5)$$

For the transversely isotropic material, $c_{11}=c_{22}$, $c_{13}=c_{23}$ and $2c_{66}=c_{11}-c_{12}$. Then, using Eq. (5) the most general Hooke’s law consists of five independent constants,

$$\begin{aligned} \sigma_{xx} &= c_{11} \frac{\partial^2 \phi}{\partial x^2} + c_{12} \frac{\partial^2 \phi}{\partial y^2} + c_{13} \lambda \frac{\partial^2 \phi}{\partial z^2}, \\ \sigma_{yy} &= c_{12} \frac{\partial^2 \phi}{\partial x^2} + c_{11} \frac{\partial^2 \phi}{\partial y^2} + c_{13} \lambda \frac{\partial^2 \phi}{\partial z^2}, \\ \sigma_{zz} &= c_{13} \frac{\partial^2 \phi}{\partial x^2} + c_{13} \frac{\partial^2 \phi}{\partial y^2} + c_{33} \lambda \frac{\partial^2 \phi}{\partial z^2}, \\ \sigma_{yz} &= 2c_{44} \frac{(1+\lambda)}{2} \frac{\partial^2 \phi}{\partial y \partial z}, & \sigma_{zx} &= 2c_{44} \frac{(1+\lambda)}{2} \frac{\partial^2 \phi}{\partial z \partial x}, \\ \sigma_{xy} &= (c_{11} - c_{12}) \frac{\partial^2 \phi}{\partial x \partial y}. \end{aligned} \quad (6)$$

These stresses are required to satisfy the three equilibrium conditions, which after simplification become

$$\begin{aligned} \frac{\partial}{\partial x} \left(c_{11} \nabla_1^2 \phi + [c_{13} \lambda + c_{44} (1 + \lambda)] \frac{\partial^2 \phi}{\partial z^2} \right) &= 0, \\ \frac{\partial}{\partial y} \left(c_{11} \nabla_1^2 \phi + [c_{13} \lambda + c_{44} (1 + \lambda)] \frac{\partial^2 \phi}{\partial z^2} \right) &= 0, \end{aligned} \quad (7)$$

and

TABLE I. Extracted values of the five elastic constants for transversely isotropic CNTRs, for two tube radii (R) within the rigid tube limit ($<25 \text{ \AA}$). The units of the constants c_{ij} and α_i are in GPa.

R (\AA)	c_{11}	c_{12}	c_{13}	c_{33}	c_{44}	(λ_1, λ_2) (p_1, p_2) (α_1, α_2)
5	68 ^a	23 ^a	11 ^b	700 ^c	7 ^d	(146, 1.0E-03) (39, 0.10) (266, -4) (266, 4.1E-04)
20	8 ^b	7 ^b	2 ^b	300 ^c	1 ^d	(100, 0.13) (797, -1)

^aFrom combined continuum/molecular mechanics model, Ref. 24.

^bFrom lattice dynamics model, Ref. 23.

^cApproximately the in-plane value in graphite, Refs. 10 and 23.

^dFrom flexural experiments, Ref. 10.

$$\frac{\partial}{\partial z} \left([c_{13}\lambda + c_{44}(1+\lambda)] \nabla_1^2 \phi + c_{33}\lambda \frac{\partial^2 \phi}{\partial z^2} \right) = 0,$$

with the notation $\nabla_1^2 \equiv \partial^2 / \partial x^2 + \partial^2 / \partial y^2$. The equilibrium equations (7) will all be satisfied as long as

$$c_{11} \nabla_1^2 \phi + [c_{13}\lambda + c_{44}(1+\lambda)] \frac{\partial^2 \phi}{\partial z^2} = 0, \quad (8a)$$

$$[c_{13}\lambda + c_{44}(1+\lambda)] \nabla_1^2 \phi + c_{33}\lambda \frac{\partial^2 \phi}{\partial z^2} = 0, \quad (8b)$$

and these two conditions become identical if we choose λ , such that

$$[c_{13}\lambda + c_{44}(1+\lambda)]^2 = c_{11}c_{33}\lambda. \quad (9)$$

This is a quadratic equation for λ with two roots

$$\lambda_{1,2} = \frac{c_{11}c_{33} - 2c_{44}(c_{13} + c_{44}) \pm \sqrt{\Delta}}{2(c_{13} + c_{44})^2}, \quad (10)$$

where $\Delta = c_{11}^2 c_{33}^2 - 4c_{11}c_{33}c_{44}(c_{13} + c_{44})$. For the remainder of the analysis, we assume that the eigenvalues λ_i ($i=1,2$) are real. This is the case for CNTRs, which are weak with respect to shear (see Table I). When $\lambda = \lambda_i$ ($i=1,2$), Eqs. (8a) and (8b) both reduce to

$$\nabla_1^2 \phi + p_i \frac{\partial^2 \phi}{\partial z^2} = 0, \quad \text{with } p_{1,2} = \frac{c_{11}c_{33} \pm \sqrt{\Delta}}{2c_{11}(c_{13} + c_{44})}. \quad (11)$$

If we then make the further transformation $z = Z_i \sqrt{p_i}$, Eq. (11) is reduced to Laplace's equation,

$$\frac{\partial^2 \phi}{\partial x^2} + \frac{\partial^2 \phi}{\partial y^2} + \frac{\partial^2 \phi}{\partial Z_i^2} = 0, \quad (12)$$

in the coordinate system (x, y, Z_i) . A more general solution can then be constructed by superposing the solutions associated with functions ϕ_1, ϕ_2 corresponding to the eigenvalues λ_1, λ_2 .

C. Solution for potential functions ϕ_1, ϕ_2

Notice that the two functions ϕ_1, ϕ_2 exist in different transformed coordinate systems, so that the point (x, y, Z) generally corresponds to two different points in the original Cartesian space, $(x, y, z/\sqrt{p_1})$ and $(x, y, z/\sqrt{p_2})$. The exception is the plane $z=0$ where $Z_1=Z_2=0$. Therefore, boundary conditions that apply on the entire $z=0$ plane can be used to seek particular solutions, i.e., Eqs. (3) and (4). To apply Eq. (4), we start with the general expression for σ_{zz} , which can be written as

$$\sigma_{zz} = c_{13} \nabla_1^2 (\phi_1 + \phi_2) + c_{33}\lambda_1 \frac{\partial^2 \phi_1}{\partial z^2} + c_{33}\lambda_2 \frac{\partial^2 \phi_2}{\partial z^2}.$$

We can use (11) to reduce this expression to the form

$$\sigma_{zz} = p_1 \alpha_1 \frac{\partial^2 \phi_1}{\partial z^2} + p_2 \alpha_2 \frac{\partial^2 \phi_2}{\partial z^2}, \quad (13)$$

where $\alpha_i = (c_{33}\lambda_i / p_i - c_{13})$. Suppose we now choose ϕ_1, ϕ_2 , such that

$$\phi_1 = A_1 \Phi(x, y, Z_1); \quad \phi_2 = A_2 \Phi(x, y, Z_2),$$

where A_1, A_2 are arbitrary constants and Φ is any harmonic function. We then have

$$\frac{\partial^2 \phi_i}{\partial z^2} = \frac{A_i}{p_i} \frac{\partial^2 \Phi}{\partial Z_i^2}(x, y, Z_i) \quad (14)$$

and on the plane $z=0$, where $Z_1=Z_2=0$,

$$\sigma_{zz} = (A_1 \alpha_1 + A_2 \alpha_2) \frac{\partial^2 \Phi}{\partial Z^2}(x, y, 0). \quad (15)$$

Then, $\sigma_{zz}=0$ for all x, y if we choose the constants A_1, A_2 , such that

$$A_1 \alpha_1 + A_2 \alpha_2 = 0. \quad (16)$$

The function Φ then retains sufficient degrees of freedom to satisfy Eq. (3). The displacement components are single derivatives of the functions ϕ . In particular, we have $u = \partial \phi / \partial r$ by analogy with (1). Thus, if we wish to obtain

constant displacements on the plane $z=0$ we shall need to start with a singular potential of order one in Φ . The appropriate harmonic function is the logarithmic potential,

$$\Phi = Z \ln[\sqrt{(r^2 + Z^2)} + Z] - \sqrt{(r^2 + Z^2)}, \quad (17)$$

(Ref. 21, Sec. 21.3). It follows that at $z=0$,

$$u_r = \frac{\partial \phi_1}{\partial r} + \frac{\partial \phi_2}{\partial r} = -(A_1 + A_2), \quad (18)$$

and the boundary condition (3) gives $-A_1 - A_2 = a_{\odot}/2$. Using Eq. (16), we get

$$A_1 = \frac{a_{\odot} \alpha_2}{2(\alpha_2 - \alpha_1)}, \quad A_2 = -\frac{a_{\odot} \alpha_1}{2(\alpha_2 - \alpha_1)}. \quad (19)$$

D. Stresses and strains

Using these values of A_1 and A_2 in Eq. (13),

$$\sigma_{zz} = \frac{a_{\odot}}{2} \frac{\alpha_1 \alpha_2}{(\alpha_2 - \alpha_1)} \sum_{i=1}^2 \left(\frac{(-1)^{i+1}}{\sqrt{r^2 + Z_i^2}} \right). \quad (20)$$

Similarly, we can combine Eqs. (6) and (11) to arrive at expressions for other stress components,

$$\sigma_{rr} = \frac{a_{\odot}}{2} \frac{\alpha_1 \alpha_2}{(\alpha_2 - \alpha_1)} \sum_{i=1,2} \frac{(-1)^{i+1}}{\alpha_i \sqrt{r^2 + Z_i^2}} \left[\frac{c_{13} \lambda_i}{p_i} - c_{12} + \frac{c_{11} - c_{12}}{r^2} (Z_i^2 - Z_i \sqrt{r^2 + Z_i^2}) \right],$$

$$\sigma_{\theta\theta} = \frac{a_{\odot}}{2} \frac{\alpha_1 \alpha_2}{(\alpha_2 - \alpha_1)} \sum_{i=1,2} \frac{(-1)^{i+1}}{\alpha_i \sqrt{r^2 + Z_i^2}} \left[\frac{c_{13} \lambda_i}{p_i} - c_{11} - \frac{c_{11} - c_{12}}{r^2} (Z_i^2 - Z_i \sqrt{r^2 + Z_i^2}) \right], \quad (21)$$

and

$$\sigma_{zr} = \frac{a_{\odot}}{2} \frac{\alpha_1 \alpha_2}{(\alpha_2 - \alpha_1)} \sum_{i=1,2} \frac{(1 + \lambda_i)(-1)^{i+1}}{\alpha_i \sqrt{p_i}} \frac{c_{44} r}{r^2 + Z_i^2 + Z_i \sqrt{r^2 + Z_i^2}}.$$

Note that the displacements associated with the IT are long range, as expected; $u_r \rightarrow r/Z$, $u_z \rightarrow \ln Z$, for $r/Z \ll 1$, and $u_r \rightarrow (1 - Z/r)$, $u_z \rightarrow \ln(Z+r)$ for $Z/r \ll 1$. In particular, the strain energy of the IT enclosed in a volume V is proportional to V . This follows from the fact that stresses and strains both vary as $1/R$, and the integral of the energy over any volume is proportional to the volume itself. *Thus, these point defects store a considerable amount of elastic energy.* The core energy where nonlinear effects dominate and the linear elastic description breaks down is restricted to a volume centered at the tip of the IT and larger than the inhomogeneity scale, i.e., a_{\odot} .

E. Application to CNTRs

Of late, there have been several studies aimed at extracting elastic constants of CNTRs.^{10,22-25} Table I summarizes

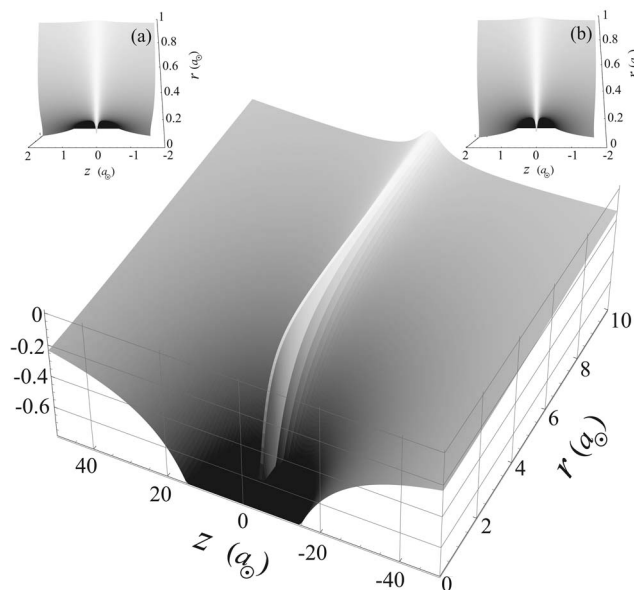


FIG. 2. Plot of $\sigma_{zz}(r, z)$. The gray scale corresponds to stress value in GPa. Insets (a) and (b) are detailed views of the dumbbell-shaped region encompassing the IT core, for $r_t=5 \text{ \AA}$ and $r_t=20 \text{ \AA}$, respectively.

the results of past experimental, simulation and theoretical studies. Based on these values, λ_i , p_i , and α_i are also tabulated. Figure 2 shows the variation of σ_{zz} for CNTRs based on nanotube radii $r_t=5 \text{ \AA}$. The stress diverges ($< -1 \text{ GPa}$) within a dumbbell-shaped (shaded dark) region centered around the IT. We expect this shape to correspond to the shape of the IT core. Fully atomistic calculations are better positioned to ascertain the details associated with the core shape, and form part of future work. Nevertheless, a comparison of the dumbbell-shaped regions for $r_t=5 \text{ \AA}$ and $r_t=20 \text{ \AA}$ suggest that the core region (and therefore the core as well as total strain energy of the IT) increases (elongated along the z direction) with decreasing tube radii (see the inset).

III. DISCUSSION AND CONCLUSIONS

Generally, the assembly of filamentous crystals is limited to finite radius aggregates. In such cases, the analysis must be modified to take into account the image forces that render the crystal surfaces traction-free. Our analysis can be easily extended to include these image forces, and is part of ongoing work. The elastic analysis also ignores the effect of temperature-dependent soft modes such as bending and twisting of filaments, which can modify the overall elastic field. As mentioned earlier, these soft modes can be safely ignored in the limit that the bend and twist persistence lengths of the individual filaments are significantly greater than the extent of the elastic displacement fields associated with the IT defect. Both nanotubes and F-actin filaments fall under this category, where the persistence lengths range from hundreds of microns (nanotubes) to even a few meters (F actin). For aggregates where soft modes become important

(e.g., liquid crystals), the elastic analysis can be refined using symmetry-breaking arguments.⁵

The weak interfilament forces are chirality and registry dependent, also ignored in the above analysis. For example, chirality results in orientational order in CNTRs.²⁷ They undergo orientational melting,⁸ wherein the two-tube unit cell with orientations φ_1 and φ_2 undergoes a first order transition to a more disordered structure consisting of orientationally decoupled tubes and random axial diffusion of twistons along the nanotube axis. In CNTRs consisting of aligned achiral (n, n) carbon nanotubes, the orientational order has a periodicity of $2\pi/n$. For $n=10$, the maximum value $U^{TT}(\Delta\varphi_{ij}^{\max}) \sim 0.5$ meV/atom and the melting temperature $T_m \approx 160$ °K. The tabulated elastic constants for CNTRs ignore the orientational order. If we account for the orientational order, the IT defect will incur an additional cost below T_m as it forms an orientational dislocation (OD) connecting the two elastic half-spaces across the $z=0$ plane (see Fig. 1).

Since the underlying orientation order consists of a unit cell of only two nanotubes, not all IT defects result in an OD. Multiple ITs with odd strength, i.e. $\chi=2k+1$, will form an OD, while even strength ITs ($\chi=2k$, $k=1, 2, 3, \dots$) preserve the orientational order across the $z=0$ plane. Furthermore, the OD can be frozen at the core of the IT, or it can spread out as an *orientational superdislocation* (OSD) via individual nanotube twistons connecting the two elastic half-spaces. The exact form of the OD will depend on the complex balance between intrinsic factors such as filament bending and torsional energies and registry-dependent energies, as well as extrinsic factors such as the IT displacement field $\mathbf{u}(u_r, u_z)$ and aspect ratio of the crystal. In one extreme scenario, the

core OD can also result in kinking of the individual filaments at the $z=0$ plane, wherein it is energetically favorable for the filament to localize the loss in registry via bending.²⁶ The other extreme case, i.e., delocalization of the loss in registry via an OSD, is more probable at crystal aspect ratios greater than the twist persistence length of the crystal. We expect this to be the generic case, as assembled nanotube tube ropes usually have aspect ratios two to three orders of magnitude.^{10,15} In this case, the orientational distribution within the OSD is expected to be coupled to $\mathbf{u}(u_r, u_z)$. The exact form of the OD is the focus of current atomic-scale studies.

In conclusion, our linear elastic analysis for an interrupted tubule (IT) in an otherwise perfectly crystalline filamentous crystal shows that the solutions can be expressed as a linear combination of two strain potentials evaluated in different coordinate mappings. The displacements are long range, implying that these defects accumulate significant strain energy. Our analysis shows that the strain energy accumulation is proportional to the volume of the aggregate itself. The analysis can easily be extended to crystalline nanotube ropes (CNTR), enabling calculation of total elastic strain energy associated with the IT defect. We find that the stresses diverge within a dumbbell-shaped core region, and the core shape is sensitive to the tube radius. We also discuss registry-dependent effects due to the IT defect, wherein an orientational dislocation is formed across odd IT defects. Thus, the electromagnetic properties of the CNTR should be significantly altered across the IT defect plane. Fully atomistic calculations are necessary to resolve the shape and structure of the core, and are the focus of ongoing studies.

¹A. Thess, R. Lee, P. Nikolaev, H. J. Dai, P. Petit, J. Robert, C. H. Xu, Y. H. Lee, S. G. Kim, A. G. Rinzler, D. T. Colbert, G. E. Scuseria, D. Tomanek, J. E. Fischer, and R. E. Smalley, *Science* **273**, 483 (1996).

²L. G. Tilney, *J. Cell Biol.* **64**, 289 (1975).

³M. F. Schmid, M. B. Sherman, P. Matsudaira, and W. Chiu, *Nature* **431**, 104 (2004).

⁴G. W. Dykes, R. H. Crepeau, and S. J. Edelstein, *Nature* **272**, 506 (1978).

⁵P. G. de Gennes and J. Prost, *The Physics of Liquid Crystals* (Oxford University Press, Oxford, 1995).

⁶C. T. Kresge, M. E. Leonowicz, W. J. Roth, J. C. Vartuli, and J. S. Beck, *Nature* **359**, 710 (1992).

⁷A. Davies, B. E. Gowen, A. M. Krebs, G. F. X. Schertler, and H. R. Saibil, *J. Mol. Biol.* **314**, 465 (2001).

⁸Y.-K. Kwon and D. Tománek, *Phys. Rev. Lett.* **84**, 1483 (2000).

⁹J. P. Hirth and J. Lothe, *Theory of Dislocations* (McGraw-Hill, New York, 1968).

¹⁰J.-P. Salvetat, G. A. Briggs, J. M. Bonard, R. R. Bacsa, A. J. Kulik, T. Stockli, N. A. Burnham, and L. Forro, *Phys. Rev. Lett.* **82**, 944 (1999).

¹¹X. F. Zhang, A. Y. Cao, Y. H. Li, C. L. Xu, J. Liang, D. H. Wu, and B. Q. Wei, *Chem. Phys. Lett.* **351**, 183 (2002).

¹²J. Liu, A. G. Rinzler, H. J. Dai, J. H. Hafner, R. K. Bradley, P. J.

Boul, A. Lu, T. Iverson, K. Shelimov, C. B. Huffman, F. Rodriguez-Macias, Y. S. Shon, T. R. Lee, D. T. Colbert, and R. E. Smalley, *Science* **280**, 1253 (1998).

¹³D. Golberg, Y. Bando, M. Mitome, K. Kurashima, N. Grobert, M. Reyes-Reyes, H. Terrones, and M. Terrones, *Chem. Phys. Lett.* **360**, 1 (2002).

¹⁴M. D. Frogley and H. D. Wagner, *J. Nanosci. Nanotechnol.* **2**, 517 (2002).

¹⁵D. A. Walters, L. M. Ericson, M. J. Casavant, J. Liu, D. T. Colbert, K. A. Smith, and R. E. Smalley, *Appl. Phys. Lett.* **74**, 3803 (1999).

¹⁶J. Hone, I. Ellwood, M. Muno, A. Mizel, M. L. Cohen, A. Zettl, A. G. Rinzler, and R. E. Smalley, *Phys. Rev. Lett.* **80**, 1042 (1998).

¹⁷K. A. William and P. C. Eklund, *Chem. Phys. Lett.* **320**, 352 (2000).

¹⁸J. Gonzalez, *Phys. Rev. B* **67**, 014528 (2003).

¹⁹N. S. Lee, D. S. Chung, and I. T. Han, *Diamond Relat. Mater.* **10**, 265 (2001).

²⁰T. C. T. Ting, *Anisotropic Elasticity: Theory and Applications* (Oxford University Press, Oxford, 1996).

²¹J. R. Barber, *Elasticity* (Kluwer Academic Press, New York, 2002).

²²J. Tersoff and R. S. Ruoff, *Phys. Rev. Lett.* **73**, 676 (1994).

²³V. N. Popov, V. E. van Doren, and M. Balkanski, *Solid State Commun.* **114**, 295 (2000).

²⁴E. Saether, S. J. V. Frankland, and R. B. Pipes, *Compos. Sci. Technol.* **63**, 1543 (2003).

²⁵L. Haiyi and M. Upmanyu, *Phys. Rev. Lett.* **94**, 065502 (2005).

²⁶A. E. Cohen and L. Mahadevan, *Proc. Natl. Acad. Sci. U.S.A.*

100, 12141 (2003).

²⁷The chiral vector relates the axis of rotation to the basis vectors of the underlying, two-dimensional graphite crystal structure. If \mathbf{a}_1 and \mathbf{a}_2 are the basis vectors of the graphite crystal, then the chiral vector can be expressed $C_h = n\mathbf{a}_1 + m\mathbf{a}_2$, where n and m are integers.